Evolution of *mir-92a* underlies natural morphological variation in *Drosophila melanogaster*

Saad Arif[1,2]*, Sophie Murat[1,2]*, Isabel Almudi[1], Maria D. S. Nunes[1], Diane Bortolamiol-Becet[6], Naomi S. McGregor[1], James M. S. Currie[1], Harri Hughes[1], Matthew Ronshaugen[3], Élio Sucena[4,5], Eric C. Lai[6], Christian Schlötterer[2], and Alistair P. McGregor[1,2+]

[1] Department of Biological and Medical Sciences, Oxford Brookes University, Gipsy Lane, Oxford, OX3 0BP, United Kingdom.

[2] Institut für Populationsgenetik, Veterinärmedizinische Universität Wien, Veterinärplatz 1, A-1210, Vienna, Austria.

[3] Faculty of Life Sciences, University of Manchester, Oxford Road, Manchester, M13 9PT, United Kingdom.

[4] Instituto Gulbenkian de Ciência, Apartado 14, 2781-901 Oeiras, Portugal.

[5] Universidade de Lisboa, Faculdade de Ciências, Departamento de Biologia Animal, Campo Grande, 1749-016 Lisboa, Portugal

[6] Sloan-Kettering Institute, 1017C Rockefeller Research Labs, 1275 York Avenue, Box 252, New York, NY, USA.

* These authors contributed equally to this work

+Author for correspondence

Running head: *mir-92a* underlies morphological evolution

Summary

Identifying the genetic mechanisms underlying phenotypic change is essential to understanding how gene regulatory networks and ultimately the genotype-to-phenotype map evolve. It is recognised that microRNAs (miRNAs) have the potential to facilitate evolutionary change[1-3], however, there are no known examples of natural morphological variation caused by evolutionary changes in miRNA expression. Therefore the contribution of miRNAs to evolutionary change remains unknown[1, 4]. *Drosophila melanogaster* subgroup species display a portion of trichome-free cuticle on the femur of the second leg called the 'naked valley'. It was previously shown that *Ultrabithorax* (*Ubx*) is involved in naked valley variation between *D. melanogaster* and *D. simulans*[5, 6]. However, naked valley size also varies among populations of *D. melanogaster* ranging from 1000 up to 30,000 μm^2. We investigated the genetic basis of intra-specific differences in the naked valley in *D. melanogaster* and found that neither *Ubx* nor *shavenbaby (svb)*[7, 8] contribute to this morphological difference. Instead, we show that changes in *mir-92a* expression underlies the evolution of naked valley size in *D. melanogaster* through repression of *shavenoid (sha)*[9]. Therefore, our results reveal a novel mechanism for morphological evolution and suggest that modulation of the expression of miRNAs potentially plays a prominent role in generating organismal diversity.

Highlights

- miR-92a represses *shavenoid* in the posterior femur to modulate the naked valley size
- Cis-regulatory changes in mir-92a causes the evolution of morphology in *Drosophila*
- Trichome pattern changes are caused by different factors in the underlying GRN
- Changes in miRNA expression might play a prominent role in phenotypic change

Results and Discussion

Intra-specific variation in the naked valley

The naked valley exhibits considerable intra-specific variation in *D. melanogaster* ranging from a trichome-free patch as small as 1000 μm^2 to a naked region of up to approximately 30,000 μm^2 (Figure 1 and Figure S1). Moreover, small and large naked valley phenotypes segregate within natural *D. melanogaster* populations (Figure 1 and Figure S1). In contrast *D. simulans* (Figure S1), *D. mauritiana* and *D. sechellia* populations, as well as *D. yakuba*, only exhibit naked valley areas at the higher end of the size range (13,000 μm^2 to 30,000 μm^2). Therefore, small naked valleys (SNVs) appear to be a derived morphological feature within *D. melanogaster*, while larger naked valleys (LNVs) are ancestral with respect to the *D. melanogaster* species subgroup.

Mapping the genetic basis of naked valley variation in D. melanogaster

It was previously shown that the Hox gene *Ubx* contributes to the difference in naked valley size between a *D. melanogaster* strain with a small naked valley and *D. simulans*[6]. Therefore, to determine if *Ubx* is also responsible for intra-specific naked valley variation in *D. melanogaster* we performed QTL mapping of naked valley size on chromosome 3 among backcross progeny from crosses between strains *st, ss, e* (LNV) and Oregon R (SNV). We found a single QTL at 88.2 centimorgans (cM) on chromosome 3 that explains up to 91% of difference in naked valley size between the two parental strains (Figure S2 and Table S1) and, using a male F1 backcrossing strategy, we determined that the remaining effect (approximately 10%) is caused by chromosome 2 ($p < 0.017$, Bonferroni corrected pair wise comparison of means). Chromosomes X and 4 have no significant effect. Our mapping thus excludes both *Ubx,* which is at 58.8 cM on chromosome 3 (Figure 2), and the X-linked gene *svb,* which is known to underlie variation in larval trichome patterns[10-12].

To verify that variation in *Ubx* is not responsible for differences in the naked valley in *D. melanogaster*, we carried out two further experiments. First, we repeated our chromosome 3

mapping strategy with two different *D. melanogaster* strains: RAL514 and *ebony (e), white ocelli (wo), rough (ro)*, which have SNVs and LNVs respectively. QTL mapping using these three recessive markers confirmed the position of a single, large effect, QTL on chromosome 3 at 79.7 to 89.7 cM (2 LOD interval), between *wo* and *ro* (Figure S2A and Table S1). Second, we generated flies with recombinant 3rd chromosomes: homozygous for the *Ubx* allele from a LNV background (Ubx^L) and homozygous for the QTL region from a SNV background (QTL^S), and vice versa (Ubx^S and QTL^L) (Figure S2B). The size of the naked valley of these flies was determined by the background from which the QTL region originated (Figure S2), and no significant effect could be attributed to *Ubx*: flies homozygous for Ubx^L and QTL^S had a small naked valley, while flies homozygous for Ubx^S and QTL^L had a large naked valley. Furthermore, the effect on naked valley area of homozygosity for QTL^L or QTL^S was consistent with the QTL mapping results (Figure S2). Our mapping results, therefore, showed that neither *Ubx* or *svb* contribute to naked valley variation in *D. melanogaster*.

To fine map the causative locus/loci in the QTL region, we took advantage of the large effect of the QTL and employed the visible flanking markers *wo* and *ro* to screen for recombinants. We measured the naked valley area of these flies and scored them for microsatellite and restriction fragment length polymorphism markers (Figure 2 and Figure S2C). This strategy allowed us to map the causative locus to a region of 25 kb that contains only four genes: part of *Npl4 ortholog*, *Succinic semialdehyde dehydrogenase (Ssadh), jing interacting gene regulatory 1 (jigr1)*, and *mir-92a* (Figure 2 and Figure S2C). *Npl4 ortholog* is thought to be the homolog of the yeast nuclear pore protein[13]. *Ssadh* encodes a ubiquitously expressed metabolic enzyme[14], while *jigr1* has been implicated in axonal guidance[15]. None of these protein-coding genes is known to be involved in trichome development. However, genome-wide analysis has shown that miR-92a and its seed-relatives have the unique ability to induce trichome loss when ectopically expressed during wing development[9, 16] (Figure S3). Therefore *mir-92a* represented a strong candidate for the evolution of the naked valley.

Functional analysis of mir-92a in naked valley development

To investigate the role of miR-92a in naked valley development, we over-expressed *UAS-mir-92a*[16] using a *heat-shock-GAL4* driver in pupal legs between 8 and 24 hours after puparium formation (APF) when the naked valley pattern is determined[6]. While control flies displayed comparatively SNVs, over expressing *mir-92a* by applying heat-shock at 8, 16 or 24 hours APF resulted in flies with progressive loss of trichomes, and therefore, larger naked valleys (Figure 3). Indeed, the posterior T2 femurs of flies heat-shocked at 24 hours APF displayed only a few trichomes (Figure 3). Driving *UAS-mir-92a* with *dac-GAL4* (which is expressed in the developing femur[17]) also resulted in the loss of trichomes and an enlarged naked valley with respect to controls (Figure 3). These experiments show that *mir-92a* can repress trichomes on the femur and variation in *mir-92a* expression modulates the size of the naked valley.

Comparison of the sequences of *mir-92a* between *D. melanogaster* strains with large and small naked valleys shows that the 22 nt sequence that constitutes the mature miRNA and flanking 200 bp immediately upstream and downstream are identical (Figure S4). This suggests that differences in the cis-regulatory region(s) (for example, enhancer sequences or splice sites) of *mir-92a* rather than changes to the primary structure of this miRNA or differential arm usage are responsible for naked valley evolution. To test this hypothesis, we carried out in situ hybridization against the primary miRNA transcripts to assess expression of *mir-92a* at 24 hours APF in the legs of *D. melanogaster* strains with LNVs and SNVs (*e, wo, ro* and Oregon R). We found that *pri-mir-92a* expression in the posterior T2 femurs is expanded in *e, wo, ro* compared to Oregon R (Figure 4). This finding is consistent with the difference in the size of the naked valleys between these strains, and therefore, supports the notion that changes in the regulation of *mir-92a* expression underlie naked valley variation.

It was previously reported that *Ubx* is involved in trichome development and the evolution of trichome patterns between species although the causative changes in *Ubx* have not yet been

identified[5, 6]. The involvement of *Ubx* in interspecific differences was most strongly evidenced by interspecific complementation tests, where flies carrying a single functional copy of *Ubx* from *D. simulans* had a larger naked valley that those with a single functional copy of *Ubx* from *D. melanogaster* in an otherwise identical genetic background[6]. However, these experiments also showed that flies with *D. melanogaster* chromosomes had consistently smaller naked valleys than those with *D. simulans* chromosomes irrespective of whether the *D. melanogaster* chromosome carried a non-functional *Ubx*, which Stern concluded was caused by the involvement of at least one other gene[6]. Since these results show that flies with *mir-92a* from *D. melanogaster* have smaller naked valleys than those with this factor from *D. simulans*, it is possible that the evolution of *mir-92a* may at least in part explain the results of these previous experiments.

miR-92a regulates naked valley size through repression of shavenoid

Searches for relevant miR-92a targets showed that the *sha* 3' UTR contains 5 highly conserved, canonical seed-match sites (Figure 4 and Figure S4). *sha* is required for trichome development[18], and its predicted degree of targeting by an individual miRNA exceeds nearly all other genes in *Drosophila*[19]. Therefore, *sha* is well-positioned to mediate changes in trichome patterning through altered miR-92a activity. We used luciferase sensor assays to show that the *sha* 3' UTR is highly and specifically repressed by miR-92a, relative to several other miRNAs that had no effect (Figure 4). Given that miRNAs often only fine-tune their targets by 20 to 30%, even in ectopic tests, the 13-fold regulation we observed indicates a potent regulatory interaction between miR-92a and *sha.*

To test if *mir-92a* regulates the size of the naked valley via *sha*, we co-expressed *UAS-mir-92a* with a *sha* construct lacking its 3'UTR[18] (Figure 3). This suppressed the naked valley and trichomes were found across the posterior T2 femur (Figure 3). These results are consistent with the interpretation that miR-92a represses trichomes via down-regulation of *sha*. In support of this, we found that *sha* was expressed in a smaller domain in the developing posterior T2 femur of the pupal

legs of flies with a LNV compared to those with a SNV (Figure 4). Therefore, our *in situ* results suggest mRNA degradation is the possible mechanism of repression, but it is possible that of translational blocking is also involved[9]. Finally, it remains possible that miR-92a also regulates other genes involved in trichome formation on the femur.

Although the exact mechanism of *sha* repression via *mir-92a* remains to be ascertained, we and others [9, 11] provide compelling evidence that the sha 3'UTR can be regulated by mir-92a leading to phenotypic effects consistent with the function of this target gene. Interestingly, *sha* is a known target of the transcription factor Svb, which is thought to act as input/output integrator to determine where trichomes will develop[10-12], and is a known hotspot for the evolution of larval trichomes[7, 8, 20, 21]. While presumably *Ubx* acts upstream of *svb* during trichome development, our results show that the modulation of the expression of a downstream gene involved in cytoskeletal organisation by a miRNA can also facilitate the evolution of trichome patterns.

Conclusions

We report here the first example of natural variation in the expression of a miRNA causing morphological change. Since the main role of miRNAs is to subtly modulate gene expression levels, variation in the expression and function of such factors appears to be an obvious mechanism to facilitate phenotypic evolution[2, 3]. While the appearance of new miRNAs and evolutionary changes in the seed sequences of these factors or the 3'UTRs of their targets have been described[22, 23], the phenotypic consequences of these genetic changes are not known. Therefore, our work represents the first experimental evidence that changes in the cis-regulatory sequences of miRNAs contributes to phenotypic evolution.

Experimental Procedures

Morphological measurements

Dissected T2 legs were mounted in Hoyer's medium and imaged under dark field (DF) or differential interference contrast (DIC) microscopy using a Leica DM5500 compound microscope and a DFC300 Camera. The area of naked valley (μm^2) was measured as the extent of the naked cuticle (without trichomes) starting at the base of the femur (red polygon in Figure 2B, C). Femur length (μm) was measured from the proximal end of the femur to the distal most bristle along the ventral margin.

Fly lines and crosses

The following stocks were used for mapping experiments: *st, ss, e* (DGRC: 101760), Oregon-R, *e, wo, ro* (BL496) and RAL514[24]. The stocks *st,ss,e* and Oregon-R were also used to generate reciprocal homozygous recombinant lines for chromosome III (Figure 3). Transgenic fly stocks used for functional analysis include: *w; dac^{GAL4}/Cyo (*referred to as *dac-GAL4*[17]*)*, *w; P(w(+mc)==GAL4-HSP70PB)* (*HS-GAL4*; a gift from Clive Wilson), *UAS-DsRed-mir-92a*[16] (referred to as *UAS-mir-92a*) *w[*]; P(w(+mC)=UAS-shaΔ3UTR GFP)3* (BL32096; referred to as *UAS-shaΔ3UTR* [18]), *bx-GAL4, ptc-GAL4* and *sd-GAL4*. All flies and crosses were performed under standard fly culture conditions. Heat shock experiments were conducted as described previously[25].

QTL mapping

Two independent backcross mapping populations were generated for QTL mapping. First we backcrossed F1 virgin female progeny (from the cross of *st, ss, e* to Oregon-R) to male *st, ss, e* flies. For the second mapping population, we backcrossed F1 hybrid virgin female progeny (from the cross of *e, wo, ro* x RAL514 to male *e, wo, ro*. Resultant backcross progeny were phenotyped for naked valley area and T2 femur length and genotyped on chromosome 3 (see Table S2 for genetic markers used). QTL analysis was performed using standard interval mapping with extended Haley-Knott regression[26] with the R package[27]. Additive allelic effects were estimated by fitting

linear models for the significant QTL. All analyses were performed with and without using femur length as a covariate.

The contribution of chromosomes X, 2 and 4 to variation in naked valley area was assayed by backcrossing male F1 progeny from a cross between Oregon R and *st, ss, e* to *st, ss, e* females, and comparing naked valley area between backcross progeny homozygous or heterozygous for each of these three chromosomes in a homozygous *st, ss, e* chromosome 3 background.

Fine scale mapping

To fine-scale map the causative locus responsible for naked valley variation in the QTL region on 3R, we generated and screened a total approximately 1000 recombinants between the QTL flanking markers *e* and *msb*, and *wo* and *ro* in backcross progeny from crosses between *D. melanogaster* strains *st, ss, e* and Oregon R, and *e, wo, ro* and Oregon R respectively. We then measured the naked valley area and femur length of recombinants and mapped the recombination breakpoints using 20 microsatellite and restriction site polymorphism markers.

Luciferase assays

The *shavenoid* 3'UTR and downstream genomic sequence was cloned into psiCHECK2 (Promega) using the cold fusion cloning kit (System biosciences) and the following primers: Cf_sha3utr_fwd; CCACCTGTTCCTGTAGCGGCCGCATTAGGCTATGCTTAAGTGC and Cf_sha3utr_rev; CCTTCACAAAGATCCCTCGAGTGAACGCAAAAGTAGCGC. Luciferase assays were carried out as described previously[28]. Briefly, cells were seeded in a 96-well plate at ~1.2 million/ml, 100 ul per well. Each well was transfected with 12.5 ng of Ub-Gal4 plasmid, 25 ng of the *UAS-mir* plasmid and 25 ng of the pSicheck derived plasmid using effectene transfection reagent (Qiagen). After 3 days, results are read using Dual-Glo luciferase assay (Promega) and a luminometer (Turner).

In situ hybridisations

In situ hybridisation was carried out using a standard protocol with DIG-labelled antisense RNA probes. 24 h APF pupae were fixed for 1 hour in 4% Formaldehyde (after pupal cases were removed). In situ hybridisations were performed with the same concentration of probe for each strain and the NBT/BCIP reaction was stopped at the same time. *Pri-mir-92a,* and *shavenoid* sequences were cloned into a TOPO PCR4 vector (Invitrogen) using GCAAAATGATGTGAGGCGTA and TCATAAGCAAAATACGAGACAT, and AGGAGGATATGGGCATTGTG and TGAACATGGGTGAACTGGAA primers respectively, following manufacturer protocol. M13 forward and reverse primers were used to linearize the DNA. T3 RNA polymerase was used to generate the DIG-labelled riboprobes.

Acknowledgments

Work in APM's group was funded by the Austrian Science Fund (FWF) (grant number M1059-B09), and Oxford Brookes University. Work in ECL's group was supported by the National Institutes of Health/National Institute of General Medical Sciences (R01-GM083300). We thank Virginie Orgogozo for fruitful discussions about the project and her comments on the manuscript.

Figure legends

Figure 1. Distribution of naked valley sizes across *D. melanogaster* populations

Posterior femurs of the second legs of *D. melanogaster* strains Oregon R (**A**) and *e, wo, ro* (**B**). Proximal is to the left and distal to the right in both panels. (**C**) Bimodal frequency distribution of naked valley phenotypes (residuals of naked valley area regressed on femur length) of 679 male flies from isofemale lines of five populations sampled from Kenya, Turkey, Spain, and North America. A minimum of three individuals was sampled for each isofemale line. Average values for strains Oregon R, RAL514 *e, wo, ro and st, ss, e* are indicated by arrows.

Figure 2. High resolution mapping of the causative locus

(**A**) The upper black bar represents chromosome 3 with the two arms (3L and 3R) indicated either side of the centromere (circle). The position of *Ubx* and selected QTL markers are shown below the bar with their positions in cM indicated above. The section of chromosome 3R highlighted by the red bar represents the 82.2 kb evolved region identified by first mapping experiment (Figure S3), which is shown expanded below, and between the broken diagonal lines, with the scale given in kb. The bars below the scale indicate the genotypes of selected recombinants with breakpoints in the 82.2 kb region (note that all flies also carried a non-recombinant chromosome from strain *e, wo, ro* that is not shown). Positions of molecular markers (Table S2) are indicated by black triangles. The number of individual flies representing each of the selected recombinant genotypes illustrated is given in parenthesis to the right. Chromosomal regions from strains *e, wo, ro* (large naked valley parental line) and Oregon R (small naked valley parental line) are indicated in black and white respectively. Chromosomal regions indicated in grey indicated DNA where the parental strain identity was not determined. The box indicates the 25 kb region that underlies naked valley variation. INV and LNV = intermediate and large naked valley phenotypes respectively.

Representative examples of T2 posterior femurs from recombinant flies with either an INV (**B**) or LNV (**C**).

Figure 3. *miR-92a* represses trichome development on the T2 femur

Uniform expression of *mir-92a* represses trichome formation progressively depending on developmental timing of over expression induced by heat shock. Panels (**A-D**) display the posterior of T2 femurs of F1 flies from the cross between *HS-GAL4* x *UAS-mir-92a*. **A** Posterior T2 femur of control F1 fly that was not heat shocked. (**A-D**) F1 flies heat shocked at 8, 16, 24 hours APF respectively. (**E**) Posterior T2 femur of the *dac-GAL4* control line. (**F**) *UAS-mir-92a* expression driven by *dac-GAL4* represses trichome formation throughout the posterior femur. (**G**) *UAS-sha*Δ*3UTR* driven by *dac-GAL4* results in the development of ectopic trichomes and removes the naked valley. (**H**) Simultaneous over expression of *UAS-sha*Δ*3UTR* and *UAS-mir-92a* using *dac-GAL4* leads to rescue of trichome formation and removes the naked valley. Transparent red shading indicates the extent of trichome-free cuticle.

Figure 4. Differential expression of *mir-92a* underlies naked valley variation through repression of *sha*

(**A**) The *sha* 3' UTR contains 5 highly conserved, canonical seed-match sites for miR-92a (see also Supplementary Figure 8). The black rectangle represents the *sha* coding region and the black line the 3' UTR. Numbering is with respect to the base pair position on chromosome 2R. Red and yellow ovals represent predicted seed-match sites for miR-92a consensus sequences shown aligned with the mature miR-92a sequence. (**B)** Luciferase sensor assays in S2 cells showed that the *sha* 3' UTR conferred >13-fold repression in response to ectopic miR-92a, but was unaffected by control miR-1 and miR-184. (**C**) Representation of the T2 pupal leg showing the femur (Fe), tibia (Ti), tarsa (Ta) and claws (Cl). Expression of *pri-mir-92a* (**D, E**) and *sha* (**F, G**), in the pupal T2 legs of strains *e, wo, ro* and Oregon R at 24 hours APF. Arrowheads indicate the femur in each picture.

Supplemental Information

Please see enclosed Supplemental Information file for figures and legends for Figures S1 to S4 and Table S1 and S2.

References

1. Li, J., and Zhang, Z. (2012). miRNA regulatory variation in human evolution. Trends Genet.
2. Niwa, R., and Slack, F.J. (2007). The evolution of animal microRNA function. Curr Opin Genet Dev *17*, 145-150.
3. Ronshaugen, M., Biemar, F., Piel, J., Levine, M., and Lai, E.C. (2005). The Drosophila microRNA iab-4 causes a dominant homeotic transformation of halteres to wings. Genes Dev *19*, 2947-2952.
4. Alonso, C.R., and Wilkins, A.S. (2005). The molecular elements that underlie developmental evolution. Nat Rev Genet *6*, 709-715.
5. Davis, G.K., Srinivasan, D.G., Wittkopp, P.J., and Stern, D.L. (2007). The function and regulation of Ultrabithorax in the legs of Drosophila melanogaster. Dev Biol *308*, 621-631.
6. Stern, D.L. (1998). A role of Ultrabithorax in morphological differences between Drosophila species. Nature *396*, 463-466.
7. Sucena, E., Delon, I., Jones, I., Payre, F., and Stern, D.L. (2003). Regulatory evolution of shavenbaby/ovo underlies multiple cases of morphological parallelism. Nature *424*, 935-938.
8. Sucena, E., and Stern, D.L. (2000). Divergence of larval morphology between Drosophila sechellia and its sibling species caused by cis-regulatory evolution of ovo/shaven-baby. Proc Natl Acad Sci U S A *97*, 4530-4534.
9. Schertel, C., Rutishauser, T., Forstemann, K., and Basler, K. (2012). Functional Characterization of Drosophila microRNAs by a Novel in vivo Library. Genetics.
10. Chanut-Delalande, H., Fernandes, I., Roch, F., Payre, F., and Plaza, S. (2006). Shavenbaby couples patterning to epidermal cell shape control. PLoS Biol *4*, e290.
11. Delon, I., Chanut-Delalande, H., and Payre, F. (2003). The Ovo/Shavenbaby transcription factor specifies actin remodelling during epidermal differentiation in Drosophila. Mech Dev *120*, 747-758.
12. Stern, D.L., and Orgogozo, V. (2008). The loci of evolution: how predictable is genetic evolution? Evolution *62*, 2155-2177.
13. DeHoratius, C., and Silver, P.A. (1996). Nuclear transport defects and nuclear envelope alterations are associated with mutation of the Saccharomyces cerevisiae NPL4 gene. Mol Biol Cell *7*, 1835-1855.
14. Rothacker, B., and Ilg, T. (2008). Functional characterization of a Drosophila melanogaster succinic semialdehyde dehydrogenase and a non-specific aldehyde dehydrogenase. Insect Biochem Mol Biol *38*, 354-366.
15. Sun, X., Morozova, T., and Sonnenfeld, M. (2006). Glial and neuronal functions of the Drosophila homolog of the human SWI/SNF gene ATR-X (DATR-X) and the jing zinc-finger gene specify the lateral positioning of longitudinal glia and axons. Genetics *173*, 1397-1415.

16. Bejarano, F., Bortolamiol-Becet, D., Dai, Q., Sun, K., Saj, A., Chou, Y.T., Raleigh, D.R., Kim, K., Ni, J.Q., Duan, H., et al. (2012). A genome-wide transgenic resource for conditional expression of Drosophila microRNAs. Development *139*, 2821-2831.
17. Heanue, T.A., Reshef, R., Davis, R.J., Mardon, G., Oliver, G., Tomarev, S., Lassar, A.B., and Tabin, C.J. (1999). Synergistic regulation of vertebrate muscle development by Dach2, Eya2, and Six1, homologs of genes required for Drosophila eye formation. Genes Dev *13*, 3231-3243.
18. Ren, N., He, B., Stone, D., Kirakodu, S., and Adler, P.N. (2006). The shavenoid gene of Drosophila encodes a novel actin cytoskeleton interacting protein that promotes wing hair morphogenesis. Genetics *172*, 1643-1653.
19. Ruby, J.G., Stark, A., Johnston, W.K., Kellis, M., Bartel, D.P., and Lai, E.C. (2007). Evolution, biogenesis, expression, and target predictions of a substantially expanded set of Drosophila microRNAs. Genome Res *17*, 1850-1864.
20. Frankel, N., Erezyilmaz, D.F., McGregor, A.P., Wang, S., Payre, F., and Stern, D.L. (2011). Morphological evolution caused by many subtle-effect substitutions in regulatory DNA. Nature *474*, 598-603.
21. McGregor, A.P., Orgogozo, V., Delon, I., Zanet, J., Srinivasan, D.G., Payre, F., and Stern, D.L. (2007). Morphological evolution through multiple cis-regulatory mutations at a single gene. Nature *448*, 587-590.
22. Zorc, M., Skok, D.J., Godnic, I., Calin, G.A., Horvat, S., Jiang, Z., Dovc, P., and Kunej, T. (2012). Catalog of microRNA seed polymorphisms in vertebrates. PLoS ONE *7*, e30737.
23. Chen, K., and Rajewsky, N. (2006). Natural selection on human microRNA binding sites inferred from SNP data. Nat Genet *38*, 1452-1456.
24. Mackay, T.F., Richards, S., Stone, E.A., Barbadilla, A., Ayroles, J.F., Zhu, D., Casillas, S., Han, Y., Magwire, M.M., Cridland, J.M., et al. (2012). The Drosophila melanogaster Genetic Reference Panel. Nature *482*, 173-178.
25. Stern, D.L. (2003). The Hox gene Ultrabithorax modulates the shape and size of the third leg of Drosophila by influencing diverse mechanisms. Dev Biol *256*, 355-366.
26. Haley, C.S., and Knott, S.A. (1992). A simple regression method for mapping quantitative trait loci in line crosses using flanking markers. Heredity (Edinb) *69*, 315-324.
27. Broman, K.W., Wu, H., Sen, S., and Churchill, G.A. (2003). R/qtl: QTL mapping in experimental crosses. Bioinformatics *19*, 889-890.
28. Okamura, K., Hagen, J.W., Duan, H., Tyler, D.M., and Lai, E.C. (2007). The mirtron pathway generates microRNA-class regulatory RNAs in Drosophila. Cell *130*, 89-100.

Figure 1

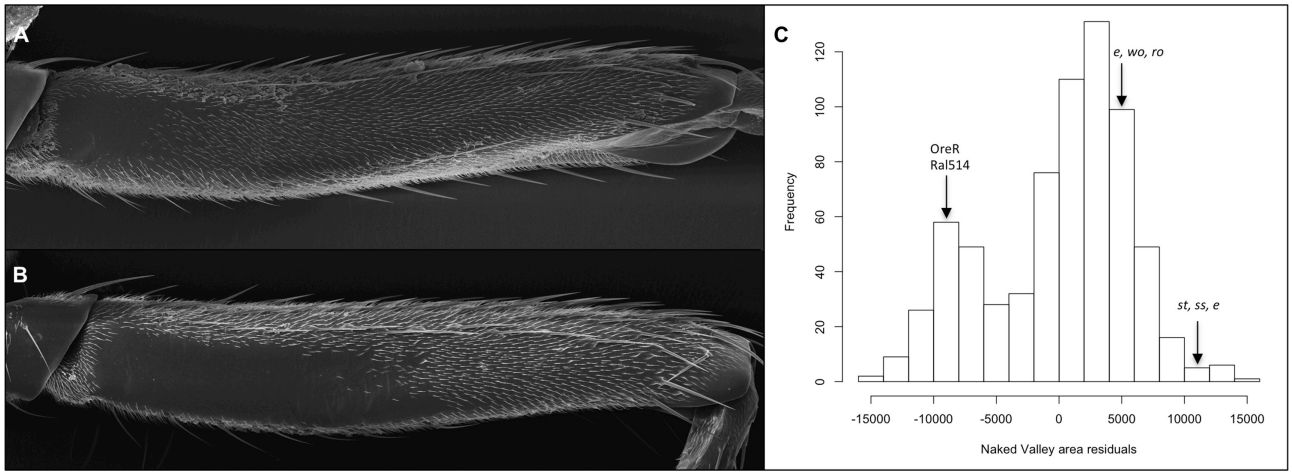

Figure 2

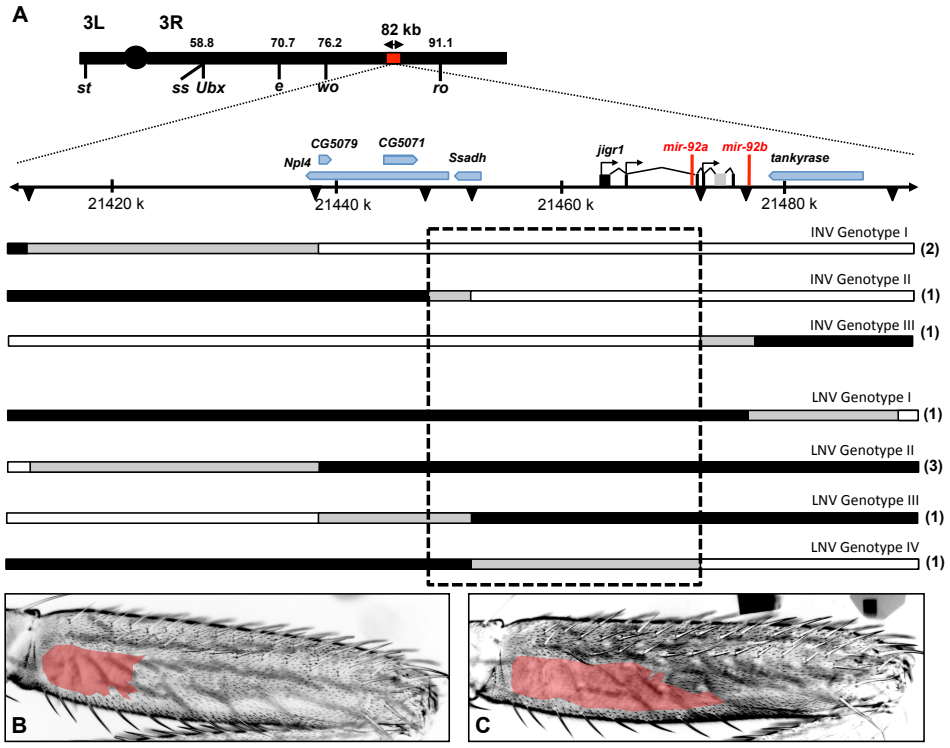

Figure 3

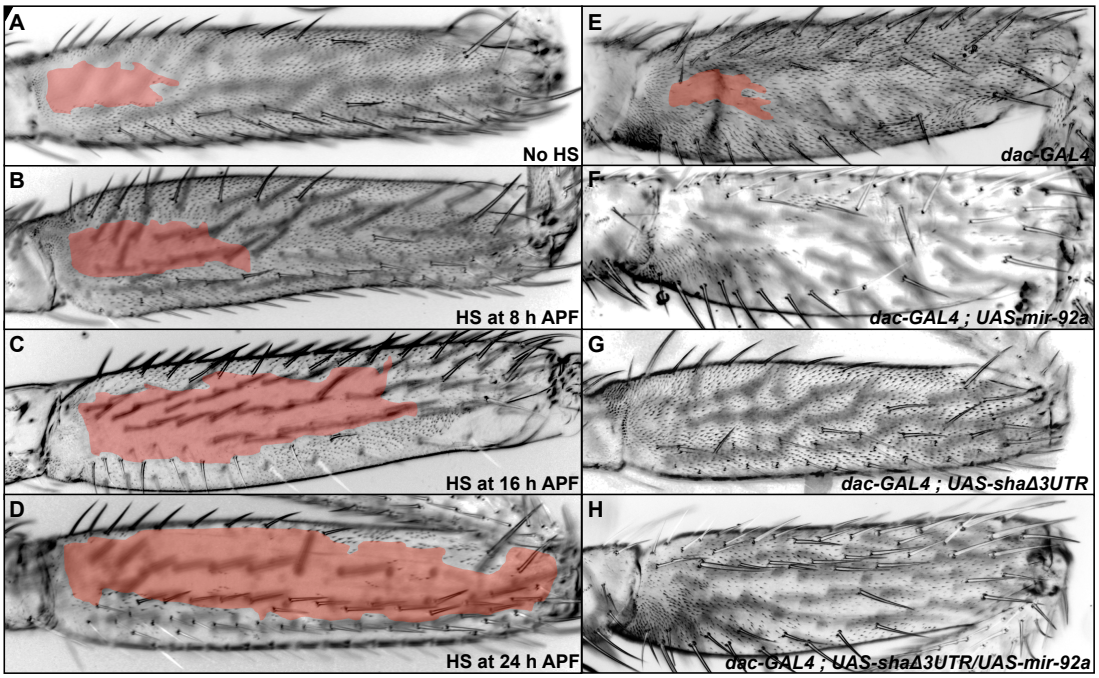

Figure 4